Journal of Chemical Technology and Metallurgy, 54, 4, 2019, 721-726

STRUCTURE AND MICROSTRUCTURE PROPERTIES OF A REFRACTORY CORDIERITE PREPARED FROM AMORPHOUS RICE HUSK SILICA RESULTING FROM PERICLACE INTRODUCTION

Simon Sembiring[1], Wasinton Simanjuntak[2], Rudy Situmeang[2]

[1] Department of Physics, Faculty of Mathematics and Natural Sciences
University of Lampung, 35145, Indonesia
[2] Department of Chemistry, Faculty of Mathematics and Natural Sciences
University of Lampung, 35145, Indonesia
E-mail: simonsembiring2@gmail.com

Received 15 March 2018
Accepted 21 February 2019

ABSTRACT

A refractory cordierite ceramic prepared from amorphous rice husk silica is modified by the addition of 5 wt. % to 20 wt. % of periclase followed by a sintering treatment at a temperature of 1230 °C. The phases, the structural changes and the microstructure characteristics of the samples are investigated by x-ray diffraction (XRD) and scanning electron microscopy (SEM). The results obtained indicate the significant effect of the periclace addition on the phase decomposition of cordierite into spinel and forsterite. The addition of periclace is found to increase the presence of forsterite and decrease that of spinel. The formation of spinel and forsterite is connected with electrical resistivity and porosity decrease but density increase.

Keywords: cordierite, periclace, silica, rice husk, structure.

INTRODUCTION

At present, rice husk is a very attractive source of reactive silica as a raw material for the preparation of ceramics, since this agriculture residue has an abundantly high silica content. This kind of silica is shown to be a good material for the synthesis of many types of materials such as pure silicon, silica nitride [1] and silicon carbide [2]. In our previous investigations reactive silica has been obtained from rice husk by a simple acid leaching. It has been used for the production of several ceramics like borosilicate [3], carbosil [4], aluminosilicates [5], mullite [6, 7] and cordierite [8 - 10].

Cordierite ($2MgO.3Al_2O_3.5SiO_2$) is a material of a low thermal expansion and dielectric constant but a high thermal and mechanical stability. It is reported that the thermal expansion of cordierite is 2.2 x 10^{-6}/°C [11], while that of other ceramic materials refer to ca 3.3 x 10^{-6}/°C [8], 1- 4 x 10^{-6}/°C [12], and 0.8-2 x10^{-6}/°C [13]. Therefore, cordierite based materials are extensively used in a broad range of applications, including catalysis, microelectronic and integrated circuit boards, membranes and refractories [14 - 17], electrical and thermal insulations [18, 19].

Several researchers study the feasibility of fabricating a dense cordierite ceramic by decreasing or increasing the content of MgO, Al_2O_3 and SiO_2. It is necessary to consider in a number of applications where a change of the crystalline phase can affect the physical, thermal, and mechanical properties of cordierite. For example, Ye et. al. [19] synthesize cordierite by decreasing Al_2O_3 mole ratio from 2 to 1.4. They find a bulk density reaching a maximum value of 2.5 kg/m^3, which is close to that of a dense cordierite ceramic. Meanwhile, an alumina addition to cordierite results in the formation of spinel, crystoballite and periclase phases [20]. Furthermore, the alumina addition increase from 10 wt. % to 20 wt. % leads to a significant increase of the density and the thermal conductivity of cordierite but electrical conductivity decrease.

The aim of this study is to identify the effect of MgO (periclace) addition on the structure and microstructure characteristics of cordierite prepared from amorphous rice husk silica. To gain insight on several basic characteristics, the structure and mictrostruture crystallisation of cordierite with periclace addition are studied by x-ray diffraction (XRD) and scanning electron microscopy (SEM).

EXPERIMENTAL

Sol silica was obtained by mixing 50 g of dried husk with 500 ml of 5 % KOH solution and boiling the mixture for 30 min in a beaker glass as reported in a previous study [**7**]. The preparation of cordierite was carried out by mixing MgO, Al_2O_3 and SiO_2 in a mass ratio of 2:2:5, correspondingly, as reported in a previous study [8]. The solid was ground using a mortar and sieved with a size of 200 meshes to obtain a powder. After that, periclace was added to the cordierite powder in a content referring to 0 wt. %, 5 wt. %, 10 wt. %, 15 wt. % and 20 wt. %. The powder was pressed in a metal die with the pressure of 2×10^4 N/m^2 to produce cylindrical pellets which were then sintered at a temperature of 1230ºC with a heating rate of 3ºC /min. The examination of the density and the porosity was done according to the Archimedes method [21]. The structure analysis was carried out using an automated Shimadzu XD-610 X-ray diffractometer, while the microstructural analysis was conducted with SEM Philips-XL. The electrical resistivity (ρ) was measured using the four-probe method.

RESULTS AND DISCUSSION

Fig. 1 shows the XRD patterns of the samples of a different periclace content sintered at a temperature of 1230ºC. The phases identified on the ground of the PDF diffraction lines with the application of the search-match method [22] show clearly the presence of α-cordierite (PDF-13-0294) with a high peak intensity 2θ = 10.5º,

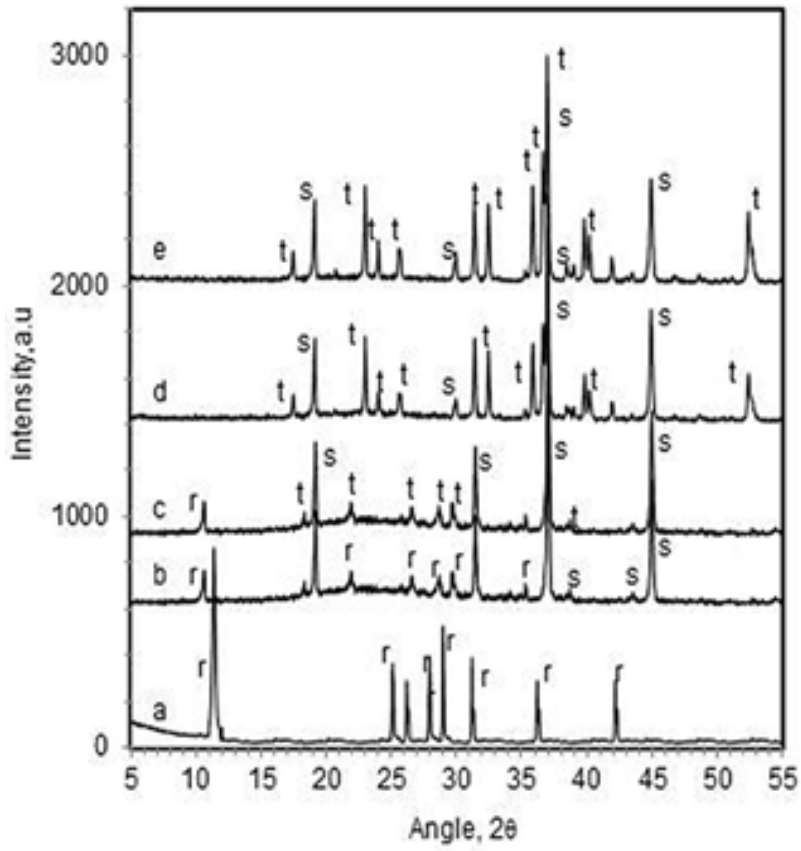

Fig. 1. X-ray diffraction patterns of samples sintered at 1230ºC whose periclace content refers to: (a) 0 %, (b) 5 %, (c) 10 %, (d)15 % and (e) 20 %; r = α-cordierite, s = spinel, t = forsterite.

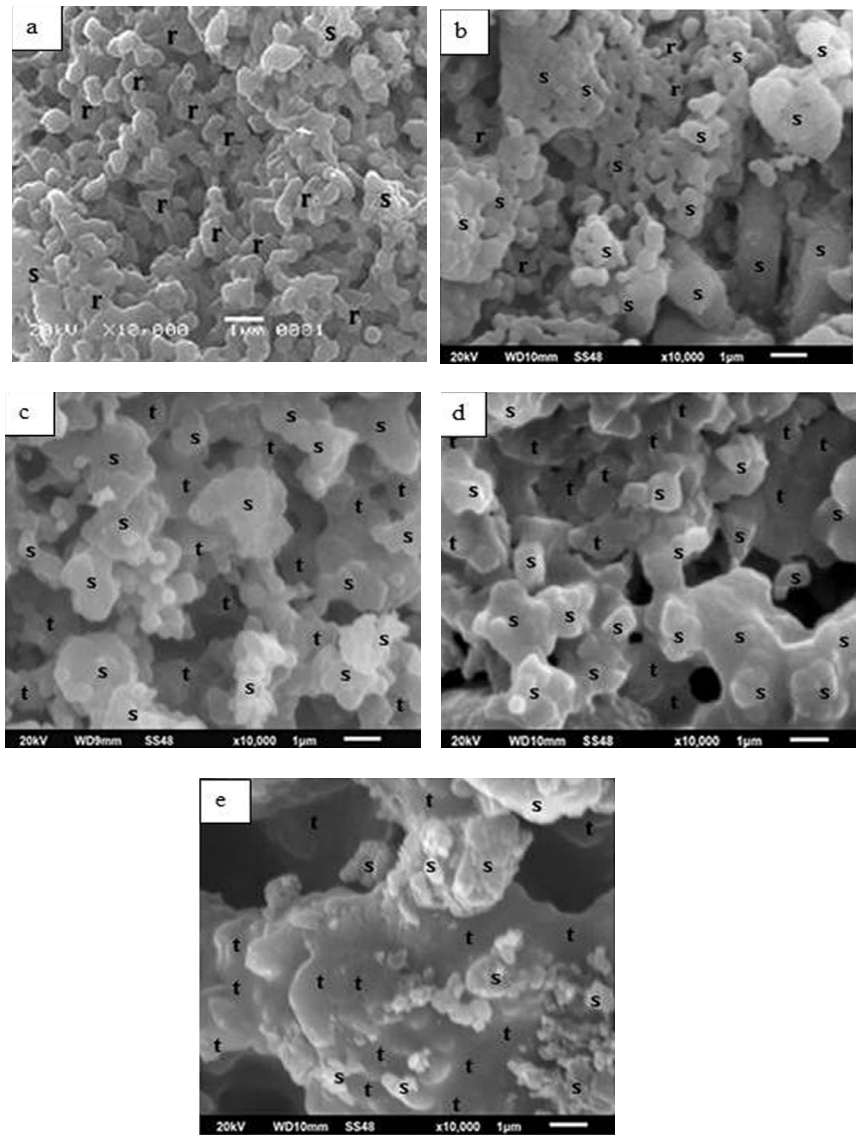

Fig. 2. SEM images of samples sintered at 1230ºC whose periclace content refers to: (a) 0 %, (b) 5 %, (c) 10 %, (d)15 % and (e) 20 %; r = α-cordierite, s = spinel, t = forsterite.

forsterite (PDF-34-0189) with 2θ = 36.55º, and spinel (PDF-21-11520) with 2θ = 36.91º. α-cordierite as a dominant phase is clearly detected in the sample containing no periclase (Fig. 1(a)). The spinel phase is well outlined, while α-cordierite presence is drastically decreased in the sample with 5 % periclace addition (Fig. 1(b)). The high presence of spinel is an indication that the 5 % periclace addition provides an intensive diffusive reaction between MgO and Al_2O_3 resulting in more spinel and less α-cordierite.

The α-cordierite is totally transformed into spinel and forsterite in case of 10 % periclace addition (Fig. 1(c)), which in turn leads to a spinel phase decrease. This presumption is in accordance with the results observed with the sample containing 15 % of periclace (Fig. 1(d)). Spinel and forsterite are detected in this case, but the phase of forsterite is evidently increased. The phases considered remain practically unchanged even in case of 20 % periclace addition (Fig. 1(e)). The spinel is formed through the interaction between AlO_6 and MgO_6 octahedral [23], while the presence of forterite results most likely from the interaction of SiO_4 and MgO_4 [24].

The surface morphologies of the samples studied are characterized by SEM. The results show a quite significant effect of the periclace addition, most likely as a result of crystallisation. The micrographs presented in

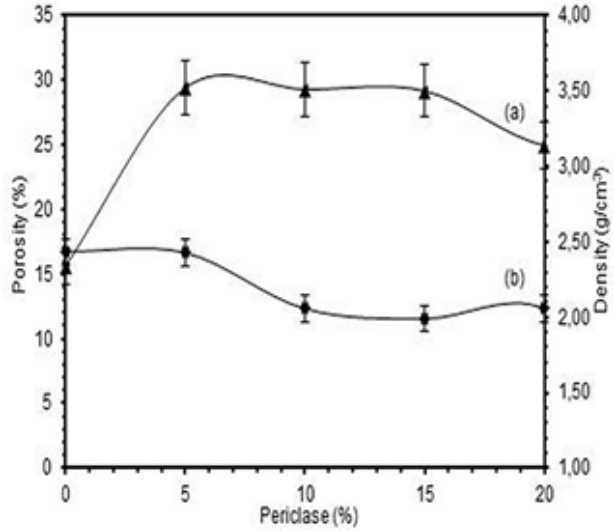

Fig. 3. Density (a) and porosity (b) as a function of the periclace content of the samples studied.

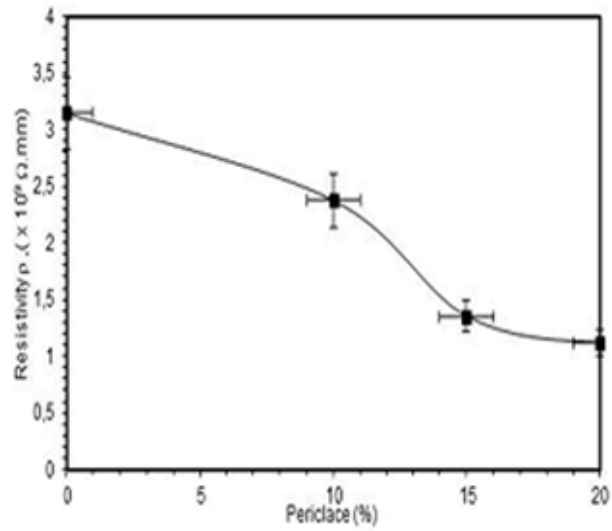

Fig. 4. Variations of the electrical resistivity as a function of the periclace content of the samples studied.

Fig. 2(a-e) illustrate the periclace effect on the size and distribution of the particles on the surface. As displayed by the images in Fig. 2(a-b), the surface morphologies of the samples are marked by the existence of particles of a different grain size and distribution.

The microstructure of the sintered sample containing no periclace (Fig. 2(a)) shows large grains with grain boundaries, while the images of the samples containing 5 % and 10 % of show no grain boundaries (Fig. 2(b-c)). In addition, it is obvious that the large grains in the sintered sample with 0 % of periclace are most likely composed of α-cordierite.This is supported by the result of the XRD analysis presented in Fig. 1(a), where α-cordierite is detected. The surface of the samples containing higher periclace content (15 % - 20 %) is occupied, as shown in Fig. 2 (d-e), by some large grains of spinel and forsterite. Both samples are marked by initiated coalescence of spinel as a result of α-cordierite crystallization. This feature suggests that with 15 % and 20 % periclace addition, α-cordierite phase continues to change leading to the formation of spinel and forsterite. This is supported by the XRD result presented in Figs 1(d,e). The formation of spinel and forsterite can be more clearly seen by inspecting the SEM micrograph of the sample containing 20 % of periclace (Fig. 2(e)).

The physical properties of the samples studied are shown in Fig. 3 and Fig. 4.

Fig. 3(a,b) shows the changes of the density and porosity of the samples as a function of their periclace content. As evident, the density of the sample containing no periclace (Fig. 3(a)) increases drastically with the periclace content increase up to 5 %. A slow decrease is observed on further periclace increase up to 20 %. Fig. 3(a) shows that the densities of the samples increase from 2.36 g/cm^3 to 3.45 g/cm^3 with periclace content increase from 0 % to 5 %. It decreases slowly and reaches a value of 3.25 g/cm^3 in 20 % periclace presence. The change of the density is most likely due to cordierite conversion into spinel and forsterite as evident from the XRD results (Fig. 1). These findings are in accordance with the results reported in refs. [25 - 27], which evidence that the density of the spinel and forsterite phases is higher than that of cordierite. The corresponding values cited there refer to 3.54 g/cm^3, 2.96 g/cm^3 and 2.3 g/cm^3. The slow decrease of the porosity (Fig. 3(b)) with periclace content increase up to 5 % is attributed to decreased formation of cordierite. The porosity continues to decrease beyond this periclace content probably indicating a domination of spinel and forsterite, smaller particles distances and smaller particle sizes in the samples as a result of the higher periclace content. This is in accordance with the surface morphologies of the samples analyzed by SEM (Fig. 2(a-e)).

Fig. 4 shows the change of the electrical resistivity of the samples as a function of the periclace addition. It is evident that the higher the periclace content corresponds to lower electrical resistivity, which implies that the samples become resistance to electricity as a result

of the increased amount of spinel and forsterite. This conclusion is supported by the XRD results presented in Fig 1. This profile demonstrates that the electrical resistivity of the samples can be controlled through spinel and periclace formation. This is very useful for adjusting the suitability of the material to specified applications such as insulators and conducting elements in electronic devices.

CONCLUSIONS

This study demonsrates the effect of periclace addition on the structure and microstructure of cordierite prepared from rice husk silica. The addition of periclace from 5 % to 20 % reveals that cordierite formation is practically undetected, while spinel and forsterite are the dominant phases present. The phase transformation is found to change the characatersitics of the samples referring to increased density because of cordierite conversion into spinel and forsterite as well as decreased porosity and electrical resistivity. The samples studied are considered insulators on the ground of the characteristics identified.

Acknowledgements

The authors acknoledge the funding provided by the Directorate of Higher Education and the Ministry of Research, Technology and Higher Education of Republic of Indonesia through 2017 Hibah Competence Research Program (Grant No: 1636/UN26.21/KU/2017).

REFERENCES

1. L. Sun, K. Gong, Silicon-based materials from rice husks and their applications, Ind. Eng. Chem. Res., 40, 2001, 5861.
2. S.K. Singh, B.C. Mohanty, S. Basu, Synthesis of SiC from rice husk in a plasma reactor, Bull. Mater. Sci., 25, 2002, 561-563.
3. S. Sembiring, Synthesis and characterization of rice husk silica based borosilicate (B_2SiO_4) ceramics by sol-gel routes, Indo. Chem., 11, 1, 2011, 85-89.
4. W. Simanjuntak, S. Sembiring, K. Sebayang, Effect of pyrolysis temperature on composition and electrical conductivity of carbosil prepared from rice husk, Indo. Chem., 12, 1, 2012, 119-125.
5. W. Simanjuntak, S. Sembiring, P. Manurung, R. Situmeang, I.M. Low, Characteristics of aluminosilicates prepared from rice husk silica and aluminum metal, Ceram. Int., 39, 8, 2013, 9369-9375.
6. S. Sembiring, W. Simanjuntak, X-ray diffraction phase analyses of mullite derived from rice husk silica", Makara. Sci., 16, 2, 2012, 77-82.
7. S. Sembiring, W. Simanjuntak, P. Manurung, D. Asmi, I.M. Low, Synthesis and characterisation of gel-derived mullite precursors from rice husk silica, Ceram. Int., 40, 5, 2014, 7067-7072.
8. S. Sembiring, W. Simanjuntak, R. Situmeang, A. Riyanto, K. Sebayang, Preparation of Refractory Cordieirite Using Amorphous Rice Husk Silica for Thermal Insulation Purposes, Ceram. Int., 42, 7, 2016, 8431-8437.
9. S. Sembiring, W. Simanjuntak, R. Situmeang, Buhani, Shella, Synthesis and characterization of Refractory Cordierite Precursors from Rice Husk Silica, Proceedings International Conferrence on Science and Science Education Faculty of Sience and Mathematics Satya Wacana Christian University Salatiga, Central Java Indonesia, 1st August 2015.
10. W. Simanjuntak, S. Sembiring, The use of Rietveld method to study the phase composition of cordierite ($Mg_2Al_4Si_5O_{18}$) Ceramics prepared from rice husk silica, Makara Sci., 15, 1, 2011, 97-100.
11. Y. Kobayashi, K. Sumi, E. Kato, Preparation of dense cordierite ceramics from magnesium compounds and kaolinite without additives, Ceram. Int.,. 26, 2000, 739-743.
12. A. Yamuna, R. Jhonson, Y.R. Mayajan, M. Lalithambika, Kaolin-Based cordierite for pollution control, Eur. Ceram. Soc. 24, 2004, 65-73.
13. S. Kurama, H. Kurama, The reaction kinetics of rice husk based cordierite ceramics, Ceram. Int., 34, 2008, 269-272.
14. P. Laokula, S. Maensirib, Synthesis, characterisation and sintering behavior of nanocrystalline cordierite ceramics, Adv. Sci. and Tech., 45, 2006, 242-247.
15. P. Scardi, N. Sartori, A. Giachello, P.P. Demaestri, F. Branda, Thermal stability of cordierite catalyst supports contaminated by Fe_2O_3, ZnO and V_2O_5, Eur. Ceram. Soc., 13, 3, 1994, 275-282.
16. L. Zhou, T. Wang, Q.T. Nguyen, J. Li, Y. Long, Z. Ping, Cordierite-supported ZSM-5 membrane: preparation and evaporation properties in the de-

hydration of water–alcohol mixture, Separat. and Purificat. Tech., 44, 3, 2005, 266-270.
17. M. Kolli, M. Hamidouche, G. Fantozzi, J. Chevalier, Elaboration and characterization of a refractory based on Algerian kaolin", Ceram. Int., 33, 8, 2007, 1435-1443.
18. J.R. González-Velasco, M.A. Gutiérrez-Ortiz, R. Ferret, A. Aranzabal, J.A. Botas, Synthesis of cordierite monolithic honeycomb by solid state reaction of precursor oxides, Mater. Sci., 34, 9, 1999, 1999-2002.
19. L. Ye, Q. Haoran, C. Xudong, Z. Ruifang, Z. Heping, Fabrication of dense cordierite ceramic through reducing Al_2O_3 mole ratio, Mater. Lett., 116, 2014, 262-264.
20. S. Sembiring, A. Riyanto, W. Simanjuntak, R. Situmeang, K. Sebayang, Effect of Alumina Addition on the Microstructure and Physical Properties of Cordierite from Amorphous Rice Husk Silica, Proceeding Nasional University of Mataram, Lombok 2016.
21. Australian Standard, 1989. Refractories and refractory material physical test methods: The determination of density, porosity and water adsorption, 1-4, 1989, 1774.
22. Powder Diffraction File (Type PDF-2), Diffraction Data for XRD Identification. International Centre for Diffraction data, 1987, PA USA.
23. R. Petrovič, Dj. Janackovič, S. Zec, S. Drmanič, L.K. Gvozdenovič, Crystallisation behavior of alkoxy-derived cordierite gels, Sol-gel Sci. Tech., 28, 1, 2003, 111-118.
24. M.C. Wilding, C.J. Benmore, J.A. Tangeman, S. Sampath, Coordination changes in magnesium silicate glasses, Eur. Phys. Lett., 67, 2, 2004,10286-10288.
25. M. Padmaraj, M. Venkateswarlu, N. Satyanarayana, Structural, electrical and dielectric properties of spinel type $MgAl_2O_4$ nanocrystalline ceramic particles synthesized by the gel combustion method, J. Ceram. Int., 41, 2015, 3178-3185.
26. K.Y. Sara, K. Lee, M. Christopher, S. Chin, C. Ramesh, Y. Tan, W.D. Teng, I. Sopyan, Characterization of Forsterite bioceramics, Adv. Mater. Res., 57, 2012, 195-198.
27. A.H. Charles, Handbook of ceramic glasses and diamonds, Mc Graw Hills, Company Inc, USA, 2011.